Title	Impact of ferrous iron dosing on iron and phosphorus solids speciation and transformation in a pilot scale membrane bioreactor
Author(s)	Wu H., Wang Y., Ikeda Atsushi, Miller C. J., Waite T. D.
Citation	Environmental Science; Water Research & Technology, 5(8),p.1400-1411
Text Version	Accepted Manuscript
URL	https://jopss.jaea.go.jp/search/servlet/search?5066199
DOI	https://doi.org/10.1039/C9EW00225A
Right	© The Royal Society of Chemistry 2019

Environmental Science
Water Research & Technology

Impact of ferrous iron dosing on iron and phosphorus solids speciation and transformation in a pilot scale membrane bioreactor

Journal:	*Environmental Science: Water Research & Technology*
Manuscript ID	EW-ART-03-2019-000225.R2
Article Type:	Paper
Date Submitted by the Author:	16-Jun-2019
Complete List of Authors:	Wu, Hao; Beijing University of Chemical Technology, Wang, Yuan; University of New South Wales Ikeda-Ohno, Atsushi; Japan Atomic Energy Agency Miller, Christopher; The University of New South Wales, School of Civil and Environmental Engineering Waite, David; The University of New South WAles, School of Civil & Environmental Engineering

Water Impact Statement

Dosing of a pilot scale MBR with a ferrous (FeII) salt for phosphorus (P) removal is shown to result in a mix of a strengite ($FePO_{4(s)}$) like mineral and phosphorous adsorbed to amorphous iron oxyhydroxides. Approaches to increasing the proportion of the strengite-like mineral form are to be encouraged given the much higher ratio of P:Fe in the biosolids produced.

Impact of ferrous iron dosing on iron and phosphorus solids speciation and transformation in a pilot scale membrane bioreactor

Hao Wu[1], Yuan Wang[1], Atsushi Ikeda-Ohno[2], Christopher J. Miller[1] and T. David Waite[1,*],

[1] Water Research Centre, School of Civil & Environmental Engineering, The University of New South Wales, Sydney 2052, Australia

[2] Collaborative Laboratories for Advanced Decommissioning Science (CLADS), Japan Atomic Energy Agency (JAEA), 2-4 Shirakata, Tokai-mura, Naka-gun, Ibaraki 319-1195, Japan

Environmental Science: Water Research & Technology

(revised version submitted May 2019)

*Corresponding author: Professor T. David Waite, Email: d.waite@unsw.edu.au

Abstract

In this study, the distributions of iron and phosphorus species in a 1.25 m^3 pilot scale submerged membrane bioreactor dosed with Fe(II) salts to either the membrane chamber or the 1st anoxic chamber were determined using X-ray absorption spectroscopy (XAS) at the iron and phosphorus K-edges. Significant differences in the distribution of Fe species were evident at the commencement of dosing depending on the chamber to which Fe(II) was dosed though these differences were much less distinct by the time steady state conditions were achieved. Both the co-precipitation of P with Fe and adsorption of phosphorus to iron oxides play important roles with regard to the removal of phosphorus from the MBR supernatant with the results of this work suggesting that P removal via formation of Fe(III)-phosphate mineral species is preferred if Fe(II) is dosed to the membrane chamber rather than the 1st anoxic chamber.

Key words: Iron, phosphorus, membrane bioreactor, X-ray absorption spectroscopy

1. Introduction

Addition of iron salts to wastewaters is widely practiced with reasons for use including odour control (via sulfide precipitation) and removal of dissolved constituents such as phosphorus (P) from solution (via either adsorption or coprecipitation) such that effluent quality targets are achieved. While Fe(III) salts have traditionally been used for P removal, we have previously shown that use of Fe(II) salts has advantages over use of Fe(III) salts including lower cost and, provided sufficient time for Fe(II) oxidation to occur, improved P removal combined with a lower propensity for membrane fouling.[1,2]

While the efficacy of using Fe(II) salts for the removal of phosphorus from wastewaters has now been well documented, much less is known about the nature of the phosphorus-containing solids formed. Theoretically, three moles of ferrous iron can precipitate two moles of phosphorus to form the mineral vivianite ($Fe_3(PO_4)_2 \cdot 8H_2O$). While this mineral may form if Fe(II) salts are dosed to anaerobic reactors or to the anoxic zone of sequential batch reactors[3] and may accumulate in sludges into which oxygen diffusion is limited,[4] ferrous species are recognized to be thermodynamically unstable under oxic conditions and would be expected to oxidize to the less soluble ferric iron on exposure to oxygen in the aerobic or membrane chambers. The extent to which ferric species are formed (and, indeed, the nature of the Fe(III) species formed) however will be dependent upon the rate of Fe(II) oxygenation with the rate of this reaction strongly dependent upon pH[5] and the presence of ligands and/or surfaces which may enhance the Fe(II) oxidation rate.[6-10] Even in the absence of oxygen, Fe(II) can be oxidized by manganese(IV) oxide[11] and, under particular conditions, nitrogen compounds such as nitrate, nitrite and nitrous oxide.[12-14] These oxygen independent pathways are typically microbially-mediated and have been reported to be of importance in activated sludge.[13,15] Wang and Waite[16] have also raised the possibility that Fe(II) could be oxidized by hydrogen peroxide

(H_2O_2) with this powerful oxidant potentially generated in membrane bioreactors through the action of oxidoreductase enzymes.

Whatever the pathway by which Fe(II) is transformed to Fe(III), the nature of the resulting Fe(III) – phosphorus species is far from certain with the possibility of formation of mineral precipitates such as strengite ($FePO_4 \cdot 2H_2O$) or, perhaps more likely in view of the rapid rate of hydrolysis of Fe(III) at circumneutral pH,[17] iron oxyhydroxides such as amorphous ferrihydrite to which orthophosphate is recognized to readily adsorb, particularly in view of their high surface area.[18] The possibility also exists that the amorphous iron oxides may transform to more crystalline phases (such as lepidocrocite, goethite and magnetite) of much lower surface area (and thus much lower capacity to adsorb phosphorus) over time[19] with this process now recognized to be enhanced by the presence of Fe(II).[20,21] However, the presence of high concentrations of ligands such as silicate, organics and phosphate which compete for iron oxyhydroxide surface sites are recognized to retard the iron oxide crystallization process[22] and, as such, the highly sorbing amorphous iron oxide phases may prevail. Many of the processes described above are presented schematically in Figure 1 in which the formation (and subsequent transformation) of the various iron and phosphorus solid phases that could form are shown.

The nature of the iron-phosphorus solid phases formed on addition of iron salts is important for a number of reasons including (i) the efficacy of the P removal process with formation of iron-phosphate minerals such as vivianite and strengite representing a much more efficient use of added iron salts than formation of iron oxyhydroxide assemblages containing adsorbed P where the molar ratio of Fe to P will be much higher than for strengite or vivinite, ii) the stability of the final disposed product with P adsorbed to amorphous iron oxyhydroxides prone to release on reductive dissolution of the iron oxyhydroxide, and iii) the ease of P recovery and/or reuse from the iron-phosphorus product formed with this likely to be

significantly more cost effective if the P is present in distinct mineral form rather than the adsorbed state.

In a previous study, iron speciation in Fe(II)- and Fe(III)-conditioned activated sludge was investigated using three 30 L bench scale MBRs fed with a synthetic wastewater[23] with the Fe and P speciation in the MBR systems to which Fe(II) and Fe(III) salts had been dosed determined once the reactors had reached steady state (after three SRTs) using X-ray absorption spectroscopy (XAS) at both Fe and P K-edges. By combining principal component analysis (PCA)/target transformation (TT) analysis and linear combination fitting (LCF) analysis, XAS has proven to be useful in enabling identification of the oxidation state and chemical speciation of elements in any sample form, including the amorphous type of solids expected in the MBR system. As a result, in the current study, the same procedures are applied to identification and quantification of the forms of Fe and P present in a 1.25 m^3 pilot-scale MBR system fed by real wastewaters and dosed with a ferrous salt for the purposes of phosphorus removal.

The results of this study extend those obtained from our previous small-scale bench scale investigations with synthetic feed to conditions typical of a full-scale wastewater submerged membrane bioreactor treatment process. In addition, rather than single time point sampling and analysis as undertaken in studies using the bench scale reactors, samples were taken here throughout the course of continuous Fe(II) addition with sampling commencing at 1 hour after Fe(II) dosing commenced through to 60 days after dosing commenced (in the case of Fe dosing to the membrane chamber) and 110 days after dosing commenced (in the case of Fe dosing to the first anoxic chamber).

2. Materials and methods

2.1 Pilot-scale MBR

A pilot scale membrane bioreactor with a working volume of 1.25 m^3 was constructed and located at Sydney Water's Bondi Wastewater Treatment Plant (WWTP) in the eastern suburbs of Sydney (Figure 2). The design parameters of the pilot plant are provided in a previous paper[1] and reproduced in Supplementary Material (see Tables S1). The primary treated effluent from Bondi WWTP was used as the feedwater to the pilot scale MBR with the study commencing in April 2012 and continuing until August 2013. The composition of this feedwater is provided in Table S2. The results of tracer studies described by Wang et al.[1] indicate that the MBR was well mixed though some short circuiting was evident on dosing to the membrane chamber. The tracer studies indicated a hydraulic residence time of 8.6-8.7 hours.

2.2 Ferrous iron dosing

A molar ratio of Fe(II):P of 2:1 was previously shown to be optimal as a balance between P removal and fouling minimisation[1] and was used here for investigation of the nature of the iron- and phosphorus-containing solids formed. 0.12 M ferrous iron solutions were prepared every two days by dissolving laboratory grade ferrous sulphate heptahydrate (Chem-Supply) in 15 L Milli-Q water containing 15 mM HCl (pH = 1.99) with this acidity sufficient to avoid oxidation of Fe(II) over the time of dosage. The solutions were pumped to the pilot reactor at a constant flowrate yielding a molar ratio of Fe(II) to orthophosphate of 2.01–4.10 during the whole experimental period (due to the fluctuations of influent phosphorus concentration). Two dosing locations were tested: i) to the membrane filtration zone from 30 October 2012 to 6 February 2012, and ii) to the primary anoxic zone from 1 May 2013 to 23 August 2013. Details regarding the pilot trials are provided in Supplementary Material (Table S3). Effluent samples from the pilot plant were collected three times per week during each experimental regime.

Total phosphorous (TP) and orthophosphate (ortho-P) concentrations were determined using standard methods (4500-P B and E).[24] The pH of the influent, effluent and suspensions in each of the chambers throughout the Fe-dosing regimes were determined routinely every few days.

2.3 Preparation and storage of activated sludge samples

Mixed liquor samples (50 mL) were collected from sampling points located at the centre of the four chambers (1st anoxic chamber, the aerobic chamber, 2nd anoxic chamber and membrane chamber). Three series of mixed liquor samples were collected: at 1 day, ~45 days and ~90 days after Fe(II) dosing. These samples were centrifuged at 4400 rpm for 10 mins. The supernatants were decanted into a dead-end filtration unit (Sterifil® Aseptic system, Millipore) with 0.8 μm membrane filters (Millex AA, Millipore) and the residual solids stored at −85 ºC for roughly 2 hrs followed by freeze-drying for at least 48 hrs to acquire final powder products. The sludge powder samples were stored in sealed polypropylene centrifuge tubes in a dark freezer (~−30 ºC) prior to the synchrotron studies and were analysed within 6 months of sample procurement.[25] Supernatant samples passing the membrane filters were further analysed to obtain the concentrations of soluble and colloidal iron and phosphorous species with size smaller than 0.8 μm.

2.4 Measurement of iron and phosphorus in the MBR effluent

Ferrous and total iron concentrations in the supernatant collected from different chambers and processed using the methods described in Section 2.3 were determined by colourimetry using ferrozine as the binding agent.[26] Details of the procedures used can be found in our previously published papers.[1,27] Ferric ion concentration was calculated by deducting the ferrous iron concentration from the total iron concentration. Phosphorous concentrations were determined using the methods described in Section 2.2.

2.5 X-ray absorption spectroscopy

Iron speciation of the sludge samples procured and stored as described in Section 2.3 was determined by X-ray absorption spectroscopy (XAS) including both X-ray absorption near-edge structure (XANES) and extended X-ray absorption fine structure (EXAFS) regions at the Fe K-edge (7112.0 eV) with X-ray absorption spectra collected on beamline 17C1 at the National Synchrotron Radiation Research Center (NSRRC) in Taiwan. For determination of the speciation of P-containing solids present in the sludge samples, XAS spectra were collected at the P K-edge (2145.5 eV) on beamline 16A1 at NSRRC. The methods of XAS data collection and analysis used here are similar to those used in our earlier studies of Fe and P speciation in bench scale membrane bioreactors[23] and are provided in Supplementary Material.

3. Results

3.1 Quantitative speciation of Fe in different chambers of the pilot scale MBR

Sludge samples were separated into two groups based on the dosing position (Group 1, Fe(II) dosed to membrane chamber; Group 2, Fe(II) dosed to 1st anoxic chamber) then PCA undertaken on each of these groups. PCA on the sixteen sludge samples in Group 1 identified two definitive principal components with a minimum IND value of 0.02428 (see Supplementary Material). The sum of these two components accounted for 72 % of the cumulative variance. The first two components satisfactorily reproduced more than half of the sample spectra in Group 1 except $Slg^{Fe(II)-ME}$_D1_1stAN, $Slg^{Fe(II)-ME}$_D60_ME, $Slg^{Fe(II)-ME}$_D60_2ndAN, $Slg^{Fe(II)-ME}$_D30_ME, $Slg^{Fe(II)-ME}$_D30_AE and $Slg^{Fe(II)-ME}$_D30_1stAN. Including four principal components improved the simulation of the spectra over inclusion of two or three principal components as shown in Supplementary Material. This is also consistent with the trend of IND values in Supplementary Material. Therefore, the four principal components were taken into account in the subsequent TT analysis in order to select

appropriate reference compounds for the system in which Fe(II) was dosed to the membrane chamber. This also limits the maximum number of reference compounds for LCF analysis to four. The results of the TT analysis are summarised in Supplementary Material. In general, reference compounds with a SPOIL value < 3 are considered to be significant components while reference compounds with a SPOIL value between 3 and 6 are considered moderately acceptable.[28] Based on this SPOIL classification, the top four Fe reference solids in Supplementary Material (i.e. ferrihydrite, strengite (as a representative of Fe(III) phosphates), lepidocrocite and Fe(III) citrate) were taken into account in the subsequent LCF analysis. Goethite, akaganéite, hematite, vivianite, pyrite and mackinawite show SPOIL values > 6 and, hence, were not considered as appropriate references for the LCF analysis. The same procedure was applied to Group 2 for which Fe(II) was dosed to the 1st anoxic chamber. Again, the results suggest that four principal components were necessary to reproduce the EXAFS spectra of the actual sludge samples with the same four significant components used in the subsequent LCF analysis. The k^3-weighted Fe K-edge EXAFS spectra for sludge samples from the pilot scale MBR with Fe(II) dosing to the membrane chamber and 1st anoxic chamber are shown in Figures S3 and S4 in Supplementary Material together with the reproduction of these spectra by four component LCF.

The results of LCF analysis of the sludge samples are provided in Table 1 and summarised in Figures 3a & b. LCF results indicate that when Fe(II) was dosed to the membrane chamber, Fe(III)-phosphate solid and ferrihydrite were the primary Fe minerals present in the MBR sludges at the initial stage of Fe dosing, accounting for 20.3–29.0% and 32.1–43.4% respectively of the Fe content of the sludge collected one hour after Fe(II) dosing ($Slg^{Fe(II)\text{-}ME}$_D0) and 36.4–45.8% and 33.8–39.4%, respectively, of the Fe content of sludge obtained one day after Fe(II) dosing ($Slg^{Fe(II)\text{-}ME}$_D1). As can be seen from Table 1, a significant portion of the Fe in the MBR system was found to be initially associated with

organic matter (as represented by the proportion of Fe(III) citrate present) with this form accounting for 36.2–42.2% and 19.8–23.2%, respectively, of the total Fe for sludges collected at one hour and one day after dosing of Fe(II) commenced. This Fe species was no longer present at extended times after Fe(II) dosing commenced. A very small fraction of Fe (0.6–3.0%) was incorporated in lepidocrocite (Table 1) after one day of Fe dosing. When the pilot-scale MBR was operated at steady state (after one SRT (equivalent to 30 days of Fe(II) dosing)), in addition to Fe(III)-phosphate solid and ferrihydrite, a significant proportion of the Fe content of the sludge samples could be assigned to lepidocrocite, accounting for 22.8–34.9% of total Fe species present (Table 1, Figure 3a). It is noteworthy that the fraction of Fe present as the Fe(III)-phosphate solid remained relatively constant throughout the whole Fe(II) dosing process with a slightly higher proportion of the Fe(III)-phosphate solid observed in the sludge samples collected from the 1st anoxic chamber initially (Figure 3a). With increase in the duration of dosing, more Fe(III)-phosphate was found in the aerobic chamber. Sludge samples collected at steady state are all characterized by a high proportion of iron oxyhydroxides (>50%) however a decrease in the total proportion of ferrihydrite present and an increase in proportion of lepidocrocite present are observed on comparing $Slg^{Fe(II)\text{-}ME}$_D30 and $Slg^{Fe(II)\text{-}ME}$_D60 samples (Figure 3a), suggesting that transformation between these two Fe species occurs within the MBR system.

The relative similarity in Fe species present in each of the four chambers at any one sampling time indicate that the system is well mixed. The small apparent differences in the proportions of the various solids present in the various chambers suggest the possibility of transformation of between the Fe species within the MBR system however much greater replication is needed in order to determine if these differences are real.

When Fe(II) was dosed to the 1st anoxic chamber, lepidocrocite formed at a very early stage of Fe dosing with the proportion of lepidocrocite mineral increasing from ~22.4% to

~41.5% with extension in duration of Fe dosing (Table 1, Figure 3b). Fe(III)-phosphate solid and ferrihydrite were also present in the sludge, accounting for 39.1–49.8% and 22.8–31.5% respectively of the Fe content at the initial stage of Fe dosing and 35.5–40.0% and 16.1–24.0% of Fe content when the MBR was operating at steady state. The highest proportion of Fe(III)-phosphate was observed in the 1st anoxic chamber throughout the whole dosing period (Table 1, Figure 3b), most likely due to the fact that the sewage inlet was also located immediately upstream of this chamber with the result that the 1st anoxic chamber had the highest supernatant phosphate concentration.[1] In accord with the results for the case above where Fe(II) was dosed to the membrane chamber, more dosed Fe precipitated in the form of ferrihydrite in the 2nd anoxic chamber when Fe(II) was dosed to the 1st anoxic chamber. Again, organically complexed Fe(III) solids were only present at the initial stage of Fe dosing (in sludge samples obtained after one day of Fe(II) dosing) but were no longer present when the MBR had reached steady state (i.e., after one SRT (equivalent to 30 days of Fe(II) dosing)). It should be mentioned that, in order to minimize the influence of the first dosing experiment (in which Fe(II) was added to the membrane chamber) on the second (in which Fe(II) was added to the 1st anoxic chamber), Fe conditioned sludge was discharged from the pilot scale MBR at the conclusion of the first dosing experiment (and before the commencement of the second experiment) over a period equivalent to three SRT (i.e., 90 days) . Despite this relatively extended period of "flushing", it appears that a residual of Fe conditioned sludge remained in the system though the total amount remaining after flushing was insignificant compared to that generated during Fe dosing.

3.2 P speciation in the Fe(II)-conditioned sludges with different dosing positions

Phosphorus K-edge XANES spectra for the inorganic and organic phosphorus reference solids used in LCF are shown in Supplementary Material. All reference spectra exhibit an intense main peak (white line) due to a $1s \rightarrow 3p$ electron transition though the peak position

varies among the different reference solids [from higher to lower energy; Fe(III)-phosphate: 2154.686 eV, $MgHPO_4$: 2154.492 eV, PO_4 adsorbed to AFO (P-adsorbed): 2154.445 eV, vivianite: 2154.431 eV, sodium triphosphate: 2154.293 eV, phytic acid: 2154.216 eV, Na_3PO_4: 2154.096 eV, ATP: 2153.970 eV, sodium polyphosphate: 2153.963 eV, and $CaHPO_4$: 2153.882 eV]. Moreover, all the reference spectra exhibit a broad peak around 2172 eV due to the EXAFS oscillation associated with the oxygen atoms of the primary coordination sphere of P atoms. Spectra for the Fe(III)-phosphate minerals and P-adsorbed possess a pre-edge feature at around 2150 eV with this pre-edge attributed to the hybridization of Fe-3*d*, O-2*p* and P-3*p* orbitals (Khare et al. 2004, Xiong et al. 2012).[29,30] Two different P-adsorbed references (PO_4 adsorbed on ferrihydrite or lepidocrocite) were also examined (data not shown here) with their P K-edge XANES spectra very similar with regard to the white-line peak and pre-edge and post-edge features, suggesting that these two PO_4 adsorbed species may not be distinguishable from one another when conducting LCF of sample spectra. Unlike $CaHPO_4$, $MgHPO_4$, vivianite, sodium triphosphate and sodium polyphosphate, each of which exhibit intricate oscillations above the absorption edge, all the sludge samples showed only one broad peak in the post-edge region up to 2180 eV.

In a manner similar to the sludge samples for Fe analysis, all the sludge samples for P analysis are separated into two groups based on the dosing positions (Group 1, Fe(II) dosed to membrane chamber; Group 2, Fe(II) dosed to 1st anoxic chamber). The PCA analysis performed on the P-XANES spectra of sludge samples in Groups 1 and 2 suggests up to six and three significant components, respectively (see Supplementary Material). Target transformation retained most of the reference solids as likely species (i.e. P-adsorbed, Fe(III)-phosphate, Na_3PO_4 (as a representative of sorbed PO_4 within Fe-free sludge flocs), ATP, phytic acid, sodium polyphosphate and sodium tripolyphosphate) except for vivianite, $CaHPO_4$ and $MgHPO_4$ that had unacceptable SPOIL values of >6. Target transformation excluded vivianite,

$CaHPO_4$ and $MgHPO_4$ as acceptable reference solids (data shown in Supplementary Material). In order to analyze the XANES spectra for Groups 1 and 2 in a comparable manner (i.e., the same number of reference spectra), the following four references were eventually selected for LCF analysis: Fe(III)-phosphate, P-adsorbed, ATP and phytic acid.

The XANES spectra for each sludge sample and their linear combination fitting results based on the selected references are provided in Supplementary Material. The proportions of each phosphorus species determined by LCF analysis to be present in the Fe(II) conditioned sludge are shown in Table 2 and Figures 3c & d. The results indicate that, before Fe dosing, the P speciation was dominated by organic P species represented by ATP. On commencing Fe(II) dosing to the membrane chamber, a large fraction of the organic P compounds diminished, either reacting with dosed Fe to form Fe(III)-phosphate or adsorbing to the surface of newly formed amorphous ferric oxyhydroxide (AFO) to form "P-adsorbed" species. Part of the initial organic P species was transformed into other types of organic P species, such as phytic acid. As found for the Fe species distributions, no prominent differences are evident with regard to P species distribution among the four different chambers. When Fe was dosed to the membrane chamber, the fraction of total P associated with organic P compounds decreased from ~55.6% during the first day of Fe dosing to 26.5% after 2 SRT (Table 2, Figure 3c). In the same period, the proportion of "P-adsorbed" species also increased, from around 20.8% to 46.3%. With regards to Fe(III)-phosphate, the total fraction of this P species fluctuates, increasing from ~23.6% to 34.1% after 1 SRT then dropping back to ~27.1% after 2 SRT (Table 2, Figure 3c).

Similar trends are evident on addition of Fe to the 1st anoxic chamber, with a large proportion of PO_4 (~50%) initially present in organically complexed form ("phytic acid") but this proportion decreasing to <30% by the time steady state conditions are reached. Concomitantly, the proportion of P adsorbed to iron oxyhydroxides increases from ~24% at

Day 1 to ~50% at Day 110 (Figure 3d). As is the case for doing to the membrane chamber, the proportion of P present as an iron phosphate mineral (Fe-P) fluctuates between about 14 and 24% over the 110 day dosing period.

4. Discussion

4.1 Iron transformations in the pilot scale MBR system with different dosing positions

In our previous study, iron speciation in Fe(II)-dosed activated sludge was investigated using three bench scale MBRs.[23] We concluded that almost all of the added Fe(II), regardless of which dosing position was chosen (anoxic or aerobic), was transformed to Fe-containing solids in the +III oxidation state in the conditioned sludges, except in the sludge-immobilized area where reductive dissolution of Fe(III) solids may have occurred. Fe(III)-phosphate species were the main Fe species present in the Fe(II)-conditioned sludge (40-50%) with lepidocrocite constituting the predominant iron oxyhydroxide phase (30-50%) and ferrihydrite accounting for only a small portion of the total Fe present (<10%), at least in the case of dosing of Fe(II). In this pilot plant study, Fe(III) minerals again dominate once the system had achieved steady state (after 2-3 SRTs) with most of the Fe present as either a strengite-like Fe(III)-phosphate mineral (38-43%) or present in the form of the crystalline iron oxide lepidocrocite (34-39%). Ferrihydrite is more important than in the bench scale study with 22-23% of the Fe in this form (Table 3).

Comparison of the pilot study results described here with those recently obtained by Li et al.[31] in studies of ferric chloride dosing to an aerated MBR is interesting where most of the iron in the sludge was present as ferrihydrite (52.4%), goethite (28.7%) and amorphous ferric phosphate (18.1%). The presence of a high proportion of lepidocrocite in our study is not surprising given that this mineral is recognized to result from oxygenation of Fe(II) salts whereas dosing with a ferric salt in the Li et al. study presumably leads to immediate formation

of ferrihydrite with a portion of this amorphous mineral apparently transforming to the more crystalline goethite over time.

Substantial additional insights are available from the pilot scale study described here as XAS analyses were also undertaken on sludge samples collected from the pilot plant after Fe(II) dosing had been continued for different periods. With Fe(II) dosed to the membrane chamber of the pilot-scale MBR, the LCF analysis showed that lepidocrocite did not form one hour after Fe(II) dosing, and less than 3% was present in samples taken after one day of Fe(II) dosing. Relatively equal amounts of Fe(III)-phosphate and ferrihydrite were present in the Fe(II)-conditioned sludge at the initial stage of dosing with the presence of significant amounts of ferrihydrite perhaps the major difference from the results obtained in the previous bench scale study (where Fe(II) was dosed to the aerobic chamber). The oxidation of dosed Fe(II) appears to be very rapid within the membrane chamber of the pilot-scale MBR with this result presumably associated with the circumneutral pH in the various chambers (see Figures S8 and S9), the relatively high level of dissolved oxygen present (>4 ppm) and the possible presence of hydrogen peroxide.[16] It is also recognized that the presence of Fe(II)-phosphate complexes such as $FePO_4^-$, $FeHPO_4$ and $FeH_2PO_4^+$ can also enhance the rate of oxidation of Fe(II).[8] The presence of ferrihydrite in the first hour of dosing is a little surprising in view of findings by Voegelin et al. [32,33] that the presence of phosphate results in the formation of Fe(III)-phosphate precipitates with iron oxides only formed after free phosphate is depleted. Apparently, in the current pilot-scale MBR system, the particular combination of pH, iron and phosphate concentrations are such that the rates of Fe interaction with OH^- and PO_4^{3-} ions are relatively evenly balanced thereby enabling the formation of both ferrihydrite and Fe(III)-phosphate minerals. The fact that Fe(II) rather than Fe(III) has been dosed in these studies may be critical to Fe(III)-phosphate mineral formation with the expected initial formation of dissolved Fe(II)-

phosphate complexes likely retarding the subsequent interaction of the Fe(III) metal centre (arising from Fe(II) oxidation) with OH^- ligands.

A notable difference in the current pilot scale study from the previous bench scale study is that at the initial stage of Fe(II) dosing, significant quantities of particulate iron-organic assemblages are present in the MBR system. In contrast to the previous bench scale study, in which only synthetic wastewater was treated as influent, primary effluent from the Bondi Sewage Treatment Plant was used in the current MBR system. It is acknowledged that Fe speciation in natural environments can be affected by not only the bioavailability of P but also pH as well as organic matter (OM) and total Fe concentrations. Indeed, the presence of organic matter is recognized to suppress the formation of Fe(III)-phosphate precipitates and/or Fe(III) oxyhydroxides and to reduce the rate and extent of polymerization/aggregation of these oxyhydroxides.[34-36] Studies also indicate that with increasing concentration of Fe, formation of Fe(III) oxyhydroxides (such as ferrihydrite) and Fe(III)-phosphate solids is preferred over formation of Fe(III)-OM assemblages. As such, the increasing dominance of Fe(III) solids over Fe(III)-OM assemblages on increasing duration of dosing of Fe(II) is to be expected as Fe accumulates in the reactor over time. The soluble OM present in the MBR will bind some of the added Fe but will remain in solution (as dissolved Fe-OM complexes) and will not be captured by the centrifugation liquid-solid separation process. A portion of the added Fe will either be internalised by bacteria or will bind to the exterior of bacterial cells (and, in both cases, be assigned to the XAS-detectable Fe-OM pool) though the amount of Fe present in these forms will be limited by the steady-state MLSS achieved in the bioreactor.

As Fe(II) dosing continues, lepidocrocite starts to form and accumulates within the MBR system. The transformation of ferrihydrite into more crystalline, thermodynamically stable minerals (such as lepidocrocite and goethite) has been reported with Fe(II) able to catalyse the structural transformation of ferrihydrite.[21] However, other investigators have shown that the

presence of Si and OM can inhibit the Fe(II)-catalysed transformation of ferrihydrite to more thermodynamically stable, crystalline Fe(III) oxyhydroxides such as goethite and lepidocrocite.[22] A recent study by Chen et al.[37] further investigated the pathways of Fe(II)-induced abiotic transformation of OM-ferrihydrite coprecipitates with different C/Fe molar ratios and Fe(II) concentrations. In addition to the finding that the extent of the transformation of ferrihydrite was modified, the abiotic transformation pathway was also altered by the presence of OM. More specifically, inhibition of goethite formation and favoured formation of lepidocrocite were evident in the systems with relatively low Fe(II) concentration (~0.2 mM Fe(II)) and in the presence of coprecipitated OM. These investigators noted that lepidocrocite served as an intermediate phase during the transformation of ferrihydrite to goethite which, in accord with the results of studies undertaken elsewhere,[20,38] limited the ongoing transformation of lepidocrocite and thus inhibited goethite formation. In the current pilot-scale MBR system, the concentration of dissolved Fe(II) in the supernatant is lower than 20 μM^1 whilst the concentration of organic matter (OM) is relatively high (with a mean influent COD of 391 mg/L). As a result, the formation of OM-ferrihydrite coprecipitates is expected and, if Fe(II)-mediated ferrihydrite crystallization occurs at all, transformation to forms more crystalline than lepidocrocite would not be expected.

While not as prevalent as is the case for Fe(II) dosing to the membrane chamber, ferrihydrite is present in the various chambers on dosing to the 1st anoxic chamber from day 1 onwards (Figure 3b). Based on results of the previous bench scale study, the formation of this amorphous iron oxyhydroxide could occur in anoxic zones due to the anaerobic oxidation of Fe(II) by nitrate-reducing bacteria present in the system.[39,40] Ferrihydrite is almost certainly formed by a more direct pathway in the aerobic and membrane chambers with the presence of oxygen in these chambers inducing the oxidation of dosed Fe(II) with subsequent rapid hydrolysis of the resultant Fe(III). A process such as this is supported by the observed decrease

in supernatant total Fe concentration (i.e., soluble plus colloidal forms of iron with size smaller than 0.8 μm) from 11.45 μM to 7.59 μM on moving from the 1st anoxic chamber to the aerobic chamber and with a further decrease to a total Fe concentration of 4.58 μM in the supernatant of the membrane chamber one hour after Fe(II) dosing.

While some previous reports suggest the formation of vivianite ($Fe_3(PO_4)_2(s)$) in Fe(II)-dosed systems,[41] LCF analysis of the Fe-EXAFS spectra indicates that the Fe(II)-conditioned sludge did not contain this Fe(II) mineral. As described below, this lack of observation of vivianite in the MBR system used here is consistent with solubility constraints.[42] When Fe dosing first commences, phosphate concentrations throughout the reactor are similar to the influent concentration (taken as 200 μM in accord with Table S8). For an Fe(II):P ratio of 2:1, this represents a dose of 400 μM Fe(II). As the influent mixes with the RAS1 stream at a recycle ratio of 300%, the effective Fe(II) dosing concentration in the primary anoxic chamber will be on the order of 100 μM as the MBR has been shown to be well mixed.[1] Speciation calculations (see Figure S10) indicate that 100 μM Fe(II) would be sufficient for vivianite formation at pH > 6 for SI = 1 however Liu et al.[43] note that an SI > 4 is required for reasonable crystal growth and, under these conditions, vivianite formation at the Fe(II) and PO_4 doses used is only likely at pH > 7. As the pH is near 7 initially for this dosing regime, it is possible that vivianite formation may have occurred initially during start up. However, if vivianite formation had occurred to any significant extent, we should have observed the presence of this mineral as vivianite oxidation is reasonably slow (see for example Figure 1 in Roldan et al.[44] where vivianite oxidation is still ongoing, even after 58 days of aeration). We thus conclude that vivianite formation, although plausible at start up, would have been observed if it did occur, and that our inability to observe it suggests no significant role for vivianite under the conditions of the studies described here.

Calculations have also been performed for the case where the MBR is operating at steady state. Under these conditions, the RAS1 stream has negligible phosphate (~3 μM according to Table S8). As such, the 200 μM PO_4 influent becomes about 50 μM PO_4 in the 1st anoxic chamber. The equivalent Fe(II) concentration remains at 100 μM, as dose is based on the influent phosphate alone. Under these conditions (see Figure S11), vivianite formation is only possible at pH > 6.2 for SI = 1 and pH > 7.5 for SI = 4. As the pH was never observed to exceed 7.5, it is thus highly improbable that the reactor was ever sufficiently supersaturated for vivianite to actually form once it reached steady state. This of course neglects the fact that Fe(II) concentrations observed are much lower than 100 μM due to the oxidation of Fe(II); indeed, they were measured to be only 1.73 μM at steady state in the primary anoxic chamber.

4.2 P speciation in the MBR system

LCF analysis of the sludge before Fe(II) dosing indicates that the P species present prior to Fe(II) dosing were principally polyphosphate and/or organic phosphate. As shown in Supplementary Material (Table S8), only a slight decrease in P concentration is observed in the wastewater supernatant on entering the MBR, with this decrease possibly due to uptake by microorganisms. Evidence from P K-edge XANES measurements that P in the sludge is mostly associated with ATP and organic P (represented by phytic acid) supports this conclusion.

Comparison of P speciation in the two Fe(II) dosed systems reveals that dosing position significantly influenced the P distributions in the sludge, particularly as conditions favouring AFO precipitation facilitate the formation of P species adsorbed to AFO surface sites. It is obvious that, whether dosing Fe(II) to either the membrane chamber or the 1st anoxic chamber, adsorption of P on Fe oxyhydroxides out-competed co-precipitation at the later stage of Fe(II) dosing (Figures 3c & d). This phenomenon is consistent with the fact that the Fe(II) dosage significantly depleted the ortho-P concentration in the mixed liquor, promoting the formation Fe oxyhydroxides and providing sufficient Fe surface sites for ortho-P adsorption. Indeed, as

mentioned above, more Fe oxyhydroxides accumulated in the MBR system during Fe(II) addition.

The finding that approximately 45% of P is present as P adsorbed to iron oxyhydroxides, 25% of P is present at a ferric phosphate mineral and the remaining 30% present as organic P on dosing an Fe(II) salt to the membrane chamber differs slightly to the results described by Li et al.[31] on dosing of an Fe(III) salt to the membrane chamber where 60% of P was adsorbed to iron oxyhydroxides, 24% was present as a ferric phosphate mineral and 16% present as organic P. Direct comparison is difficult in view of the likely differences in wastewater composition though the higher proportion of P adsorbed to iron oxyhydroxides in the Fe(III) dosing case is to be expected given the higher proportion of Fe present as amorphous iron oxyhydroxides than is the case on Fe(II) dosing as described here.

Linear combination fitting indicated that phytic acid, an organic P species, was the main component (>50% of total P) in the "iron-free" sludges. The fraction of total P determined to be phytic acid in Fe(II) conditioned sludge eventually decreased from 50-55% of total P at day 1 to 25–36% of total P at day 110. While phytic acid may indeed be present as it is recognized to be the product of residential and industrial wastewater treatment and is widely spread in environmental soils and sediments,[45,46] other organic P species may yield similar XANES spectra as phytic acid. However, it is uncertain that the introduction of additional organic P references would improve the XANES fitting due to the lack of distinguishable pre-edge or post-edge features of the XANES spectra of organic/inorganic P species.[47] Moreover, the XANES spectrum of phytic acid could be fitted using the spectra of orthophosphate diesters or phospholipids[48] suggesting that XANES spectroscopy at the P K-edge is not the most sensitive technique for organic P identification.

5. Conclusions

Results of analysis of the nature of Fe and P species present within sludge samples from a pilot scale 1.25 m^3 membrane bioreactor treating real wastewaters indicate that, at steady state and depending on the dosing location, approximately 20-25% of the phosphorus is present as a 1:1 Fe(III) phosphate mineral similar to strengite ($FePO_4$(s)), 40-50% present as P adsorbed to iron oxides and the remainder present as organic-P assemblages. Formation of the Fe(III) phosphate mineral is enhanced somewhat by dosing Fe(II) to the membrane chamber with this form recognized to be the most effective for P removal and recovery in view of the 1:1 P:Fe stoichiometry of this mineral, particularly in comparison to P adsorbed to iron oxides for which the P:Fe stoichiometry will be much lower. Further trials should be undertaken to determine the conditions under which the proportion of 1:1 Fe(III)-phosphate solids present can be increased even further in view of the much greater effective use of dosed Fe and, in all probability, less severe membrane fouling in view of the more crystalline nature of this product. There would also be value in using complementary methods (to XAS) of characterising the Fe- and P-containing solids present with techniques such as Mossbauer spectroscopy of particular value in differentiating between different Fe minerals.

Acknowledgement

Funding provided by the Australian Research Council, Water Research Australia, Sydney Water and Beijing Origin Water through ARC-Linkage project LP100100056 is gratefully acknowledged. The authors would also like to acknowledge the support provided by plant operators at Bondi WWTP and Beijing OriginWater for provision of membranes. XAS analyses were undertaken at the Taiwan National Synchrotron Radiation Research Center (Proposals No. 2015-1-094-1 and 2015-1-094-2). Jeng-Lung Chen, Ling-Yun Jang, Jyh-Fu Lee and Bing-Jian Su of the NSRRC are acknowledged for their technical support.

References

1. Y. Wang, K.H. Tng, H. Wu, G. Leslie and T.D. Waite, Removal of phosphorus from wastewaters using ferrous salts – a pilot scale membrane bioreactor study, *Water Res.*, 2014, **57**, 140-150.
2. Z. Zhang, Y. Wang, G.L. Leslie and T.D. Waite, Effect of ferric and ferrous iron addition on phosphorus removal and fouling in submerged membrane bioreactors, *Water Res.*, 2015, **69**, 210-222.
3. J. Liu, X. Cheng, X. Qi, N. Li, J. Tian, B. Qiu, K. Xu and D. Qu, Recovery of phosphate from aqueous solutions via vivianite crystallization: thermodynamics and influence of pH, *Chem. Eng. J.*, 2018, **349**, 37-46.
4. P. Wilfert, A. Mandalidis, A.I. Dugulan, K. Goubitz, L. Korving, H. Temmink, G.J. Witkamp and M.C.M. Van Loosdrecht, Vivianite as an important iron phosphate precipitate in sewage treatment plants, *Water Res*., 2016, **104**, 449-460.
5. A.N. Pham and T.D. Waite, Oxygenation of Fe(II) in the presence of citrate in aqueous solutions at pH 6.0−8.0 and 25 °C: Interpretation from an Fe(II)/citrate speciation perspective, *J. Phys. Chem. A*, 2008, **112**, 643-651.
6. A.M. Jones, P.J. Griffin and T.D. Waite, Ferrous iron oxidation under acidic conditions: Effect of citric acid, EDTA and fulvic acid, *Geochim. Cosmochim. Acta.*, 2015, **160**, 117-131.
7. A.M. Jones, P.J. Griffin, R.N. Collins and T.D. Waite, Ferrous iron oxidation under acidic conditions – The effect of ferric oxide surfaces, *Geochim. Cosmochim. Acta.*, 2015, **156**, 241-241.
8. Y. Mao, A.N. Pham, A.L. Rose and T.D. Waite, Influence of phosphate on the oxidation kinetics of nanomolar Fe(II) in aqueous solution at circumneutral pH, *Geochim. Cosmochim. Acta.*, 2011, **75**, 4601-4610.
9. A.L. Rose and T.D. Waite, Kinetic model for Fe(II) oxidation in seawater in the absence and presence of natural organic matter, *Environ. Sci. Technol.*, 2002, **36**, 433-444.
10. J.M. Santana-Casiano, M. González-Dávila and F.J. Millero, Oxidation of nanomolar levels of Fe(II) with oxygen in natural waters, *Environ. Sci. Technol.*, 2005, **39**, 2073-2079.
11. K.H. Nealson and D. Saffarini, Iron and manganese in anaerobic respiration: environmental significance, physiology, and regulation, *Annu. Rev. Microbiol.*, 1994, **48**, 311-343.
12. R.J. Buresh and J.T. Moraghan, Chemical reduction of nitrate by ferrous iron, *J. Environ. Qual.*, 1976, **5**, 320-325.
13. J.L. Nielsen and P.H. Nielsen, Microbial nitrate-dependent oxidation of ferrous iron in activated sludge, *Environ. Sci. Technol.*, 1998, **32**, 3556-3561.
14. K.L. Straub, M. Benz, B. Schink and F. Widdel, Anaerobic, nitrate-dependent microbial oxidation of ferrous iron, *Appl. Environ. Microbiol.*, 1996, **62**, 1458-1460.
15. S. Hauck, M. Benz, A. Brune and B. Schink, Ferrous iron oxidation by denitrifying bacteria in profundal sediments of a deep lake (Lake Constance), *FEMS Microbiol. Ecol.*, 2001, **37**, 127-134.
16. W.-M. Wang and T.D. Waite, Iron speciation and iron species transformation in activated sludge membrane bioreactors, *Water Res.*, 2010, **44**, 3511-3521.
17. A.N. Pham, A.L. Rose, A.J. Feitz and T.D. Waite, Kinetics of ferric iron precipitation in aqueous solutions at pH 6.0 – 9.5 and 25°C, *Geochim. Cosmochim. Acta.*, 2006, **70**, 640-650.
18. Y. Mao, A.N. Pham, Y. Xin and T.D. Waite, Effects of pH, floc age and organic compounds on the removal of phosphate by pre-polymerized hydrous ferric oxides, *Sep. Purif. Technol.*, 2012, **91**, 38-45.
19. R.M. Cornell, R. Giovanoli and W. Schneider, Review of the hydrolysis of iron(III) and the crystallization of amorphous iron(III) hydroxide hydrate, *J. Chem. Technol. Biotechnol.*, 1989, **46**, 115-134.
20. H.D. Pedersen, D. Postma, R. Jakobsen and O. Larsen, Fast transformation of iron oxyhydroxides by the catalytic action of aqueous Fe(II), *Geochim. Cosmochim. Acta.*, 2005, **69**, 3967-3977.

21. D.D. Boland, R.N. Collins, C.J. Miller, C.J. Glover and T.D. Waite, Effect of solution and solid-phase conditions on the Fe(II)-accelerated transformation of ferrihydrite to lepidocrocite and goethite, *Environ. Sci. Technol.*, 2014, **48**, 5477-5485.
22. A.M. Jones, R.N. Collins, J. Rose and T.D. Waite, The effect of silica and natural organic matter on the Fe (II)-catalysed transformation and reactivity of Fe (III) minerals, *Geochim. Cosmochim. Acta.*, 2009, **73**, 4409-4422.
23. H. Wu, A. Ikeda-Ohno, Y. Wang and T.D. Waite, Iron and phosphorus speciation in Fe-conditioned membrane bioreactor activated sludge, *Water Res.*, 2015, **76**, 213-226.
24. *Standard methods for the examination of water and wastewater*, 22nd ed., American Public Health Association (APHA), American Water Works Association, and Water Environment Federation, Washington, DC, 2012
25. M. Oakes, R.J. Weber, B. Lai, A. Russell and E.D. Ingall, Characterization of iron speciation in urban and rural single particles using XANES spectroscopy and micro X-ray fluorescence measurements: investigating the relationship between speciation and fractional iron solubility, *Atmos. Chem. Phys.*, 2012, **12**, 745-756.
26. E. Viollier, P.W. Inglett, K. Hunter, A.N. Roychoudhury and P. Van Cappellen, The ferrozine method revisited: Fe(II)/Fe(III) determination in natural waters, *Appl. Geochem.*, 2000, **15**, 785-790.
27. Y. Wang, G.L. Leslie and T.D. Waite, Impact of iron dosing of membrane bioreactors on membrane fouling, *Chem. Eng. J.*, 2014, **252**, 239-248.
28. E.R. Malinowski, *Factor Analysis in Chemistry*, 3rd ed., John Wiley and Sons, Inc., 2002.
29. N. Khare, D. Hesterberg, S. Beauchemin and S.-L. Wang, XANES determination of adsorbed phosphate distribution between ferrihydrite and boehmite in mixtures, *Soil. Sci. Soc. Am. J.*, 2004, **68**, 460-469.
30. W. Xiong, J. Peng and Y. Hu, Use of X-ray absorption near edge structure (XANES) to identify physisorption and chemisorption of phosphate onto ferrihydrite-modified diatomite, *J. Colloid Interface Sci.*, 2012, **368**, 528-532.
31. R.H. Li, J.L. Cui, X.D. Li and X.Y. Li, Phosphorus removal and recovery from wastewater using Fe-dosing bioreactor and co-fermentation: investigation by X-ray absorption Near-Edge Structure spectroscopy, *Environ. Sci. Technol.*, 2018, **52**, 14119-14128.
32. A. Voegelin, R. Kaegi, J. Frommer, D.Vantelon and S.J. Hug, Effect of phosphate, silicate, and Ca on Fe(III)-precipitates formed in aerated Fe(II)- and As(III)-containing water studied by X-ray absorption spectroscopy, *Geochim. Cosmochim. Acta.*, 2010, **74**, 164-186.
33. A. Voegelin, A.-C. Senn, R. Kaegi, S.J. Hug and S. Mangold Dynamic Fe-precipitate formation induced by Fe(II) oxidation in aerated phosphate-containing water, *Geochim. Cosmochim. Acta.*, 2013, **117**, 216-231.
34. T. Karlsson and P. Persson, Coordination chemistry and hydrolysis of Fe(III) in a peat humic acid studied by X-ray absorption spectroscopy, *Geochim. Cosmochim. Acta.*, 2010, **74**, 30-40.
35. T. Karlsson and P. Persson, Complexes with aquatic organic matter suppress hydrolysis and precipitation of Fe(III), *Chem. Geol.*, 2012, **322–323**, 19-27.
36. A. Sundman, T. Karlsson, S. Sjöberg and P. Persson, Impact of iron–organic matter complexes on aqueous phosphate concentrations, *Chem. Geol.*, 2016, **426**, 109-117.
37. C. Chen, R. Kukkadapu and D.L. Sparks, Influence of coprecipitated organic matter on Fe^{2+}(aq)-catalyzed transformation of ferrihydrite: implications for carbon dynamics, *Environ. Sci. Technol.*, 2015, **49**, 10927-10936.
38. C.M. Hansel, S.G. Benner and S. Fendorf, Competing Fe(II)-induced mineralization pathways of ferrihydrite, *Environ. Sci. Technol.*, 2005, **39**, 7147-7153.
39. K.L. Straub, M. Benz and B. Schink, Iron metabolism in anoxic environments at near neutral pH, *FEMS Microbiol. Ecol.*, 2001, **34**, 181-186.
40. K.L. Straub, M. Hanzlik and B.E.E. Buchholz-Cleven, The use of biologically produced ferrihydrite for the isolation of novel iron-reducing bacteria, *Syst. Appl. Microbiol.*, 1998, **21**, 442-449.
41. E. Frossard, J.P. Bauer and F. Lothe, Evidence of vivianite in $FeSO_4$-flocculated sludges, *Water Res.*, 1997, **31**, 2449-2454.

42. A. Al-Borno and M.B. Tomson, The temperature dependence of the solubility product constant of vivianite, *Geochim. Cosmochim. Acta.*, 1994, **58**, 5373-5378.
43. J. Liu, X. Cheng, X. Qi, N. Li, J.B. Tian, B. Qiu, K.N. Xu and D. Qu, Recovery of phosphate from aqueous solutions via vivianite crystallization: Thermodynamics and influence of pH, *Chem. Eng. J.*, 2018, **349**, 37-46.
44. R. Roldan, V. Barron and J. Torrent, Experimental alteration of vivianite to lepidocrocite in a calcareous medium, *Clay Miner.*, 2002, **37**, 709–718.
45. N. Fagel, L.Y. Alleman, L. Granina, F. Hatert, E. Thamo-Bozso, R. Cloots and L. André, Vivianite formation and distribution in Lake Baikal sediments, *Glob. Planet. Change*, 2005, **46**, 315-336.
46. C.J. De Groot and H.L. Golterman, On the presence of organic phosphate in some Camargue sediments: evidence for the importance of phytate, *Hydrobiologia*, 1993, **252**, 117-126.
47. B.L. Turner, L.M. Condron, S.J. Richardson, D.A. Peltzer and V.J. Allison, Soil organic phosphorus transformations during pedogenesis, *Ecosystems*, 2007, **10**, 1166-1181.
48. J.M. Seiter, K.E. Staats-Borda, M. Ginder-Vogel and D.L. Sparks, XANES spectroscopic analysis of phosphorus speciation in alum-amended poultry litter, *J. Environ. Qual.*, 2008, **37**, 477-485.

Table 1. Summary of Fe mineral distribution (%) calculated by linear combination fitting analysis of Fe K-edge EXAFS spectra for sludges collected from pilot scale MBR.

Group 1:Fe dosed to membrane chamber

	Sample	Fractions (%)[a]				R factor	Reduced χ^2
		Fe(III)-phosphate	Ferrihydrite	Lepidocrocite	Fe(III) citrate		
Day 0 (1hr)	**$Slg^{Fe(II)-ME}$_D0_1stAN**	25.8	32.1	0	42.2	0.02632	29.3401
	$Slg^{Fe(II)-ME}$_D0_AE	24.8	36.8	0	38.5	0.03998	41.1210
	$Slg^{Fe(II)-ME}$_D0_2ndAN	20.3	43.4	0	36.2	0.03674	34.3645
	$Slg^{Fe(II)-ME}$_D0_ME	29.0	34	0	37.1	0.04296	44.7126
Day 1	**$Slg^{Fe(II)-ME}$_D1_1stAN**	45.8	33.8	0.6	19.8	0.03189	31.9643
	$Slg^{Fe(II)-ME}$_D1_AE	40.7	37.5	1.5	20.4	0.03588	34.3438
	$Slg^{Fe(II)-ME}$_D1_2ndAN	36.4	39.4	3.0	21.2	0.03787	38.3736
	$Slg^{Fe(II)-ME}$_D1_ME	39.8	35.6	1.4	23.2	0.03213	31.3432
Day 30	**$Slg^{Fe(II)-ME}$_D30_1stAN**	42.1	34.1	23.8	0	0.02474	24.3852
	$Slg^{Fe(II)-ME}$_D30_AE	45.6	27.4	27.1	0	0.02780	29.0858
	$Slg^{Fe(II)-ME}$_D30_2ndAN	39.4	35.7	25.0	0	0.03175	29.6174
	$Slg^{Fe(II)-ME}$_D30_ME	44.8	30.7	24.6	0	0.02266	22.1020
Day 60	**$Slg^{Fe(II)-ME}$_D60_1stAN**	44.5	24.2	31.3	0	0.02381	25.9483
	$Slg^{Fe(II)-ME}$_D60_AE	45.1	19	35.9	0	0.02421	27.8629
	$Slg^{Fe(II)-ME}$_D60_2ndAN	40.0	26.2	33.8	0	0.03044	32.1350
	$Slg^{Fe(II)-ME}$_D60_ME	44.0	21.9	34.1	0	0.02763	30.6347

[a] Statistical fit uncertainties generated from Athena for individual fractions were typically around 2-5 %.

Group 2: Fe dosed to 1st anoxic chamber

	Sample	Fractions (%)[a]				R factor	Reduced χ^2
		Fe(III)-phosphate	Ferrihydrite	Lepidocrocite	Fe(III) citrate		
Before dosing	$Slg^{no\ dosing}$_ME	34.2	34	13.1	18.7	0.06080	62.3348
Day 1	$Slg^{Fe(II)-1stAN}$_D1_1stAN	49.8	22.8	20.2	7.3	0.03183	33.9766
	$Slg^{Fe(II)-1stAN}$_D1_AE	44.6	25.7	21.8	7.8	0.02537	25.8329
	$Slg^{Fe(II)-1stAN}$_D1_2ndAN	42.9	27.9	23.1	6.1	0.03420	35.3674
	$Slg^{Fe(II)-1stAN}$_D1_ME	39.1	31.5	24.5	4.9	0.04640	47.2123
Day 60	$Slg^{Fe(II)-1stAN}$_D60_1stAN	38.6	20.4	41.1	0	0.01565	17.4115
	$Slg^{Fe(II)-1stAN}$_D60_AE	37.6	20.1	42.3	0	0.01501	16.8824
	$Slg^{Fe(II)-1stAN}$_D60_2ndAN	35.5	20.9	43.6	0	0.02171	25.1669
	$Slg^{Fe(II)-1stAN}$_D60_ME	37.5	16.1	46.4	0	0.01812	21.8157
Day 110	$Slg^{Fe(II)-1stAN}$_D110_1stAN	40.0	22.1	38.0	0	0.01447	15.8038
	$Slg^{Fe(II)-1stAN}$_D110_AE	37.7	23.9	38.5	0	0.01713	18.5502
	$Slg^{Fe(II)-1stAN}$_D110_2ndAN	36.8	24.0	39.2	0	0.01208	12.8227
	$Slg^{Fe(II)-1stAN}$_D110_ME	38.3	19.2	42.5	0	0.01374	15.9373

[a] Statistical fit uncertainties generated from Athena for individual fractions were typically around 2-5 %.

Table 2. Summary of P species distribution (%) calculated by linear combination fitting analysis of P K-edge XANES data for sludge collected from pilot scale MBR.

Group 1:Fe dosed to membrane chamber

Sample		Fractions (%)[a]				R factor	Reduced χ^2
		Fe(III)-phosphate	P-adsorbed	ATP	Phytic acid		
Before dosing	**$Slg^{no\ dosing}$_ME**	n.d.	n.d.	100.0	n.d.	0.009279	1.457655
Day 1	**$Slg^{Fe(II)-ME}$_D1_1stAN**	27.5	17.4	n.d.	55.1	0.006744	1.011248
	$Slg^{Fe(II)-ME}$_D1_AE	23.9	22.1	n.d.	54.1	0.006021	0.970338
	$Slg^{Fe(II)-ME}$_D1_2ndAN	20.6	23.3	n.d.	56.2	0.008035	1.302862
	$Slg^{Fe(II)-ME}$_D1_ME	22.5	20.4	n.d.	57.1	0.005647	0.91702
Day 30	**$Slg^{Fe(II)-ME}$_D30_1stAN**	34.6	29.6	n.d.	36.0	0.000548	0.082638
	$Slg^{Fe(II)-ME}$_D30_AE	34.5	30.8	n.d.	34.7	0.000574	0.089142
	$Slg^{Fe(II)-ME}$_D30_2ndAN	33.1	31.5	n.d.	35.3	0.000531	0.087349
	$Slg^{Fe(II)-ME}$_D30_ME	34.4	31.0	n.d.	34.6	0.000528	0.084821
Day 60	**$Slg^{Fe(II)-ME}$_D60_1stAN**	27.1	45.5	n.d.	27.4	0.000268	0.042035
	$Slg^{Fe(II)-ME}$_D60_AE	27.8	46.5	n.d.	25.7	0.000231	0.037398
	$Slg^{Fe(II)-ME}$_D60_2ndAN	26.2	46.9	n.d.	26.9	0.001792	0.248952
	$Slg^{Fe(II)-ME}$_D60_ME	27.5	46.4	n.d.	26.1	0.000280	0.044768

[a] Statistical fit uncertainties generated from Athena for individual fractions were typically around 2-5 %. "n.d.": not detected.

Group 2: Fe dosed to 1st anoxic chamber

	Sample	Fractions (%)[a]				R factor	Reduced χ^2
		Fe(III)-phosphate	P-adsorbed	ATP	Phytic acid		
Before dosing	$Slg^{no\ dosing}$ _ME'	11.3	6.0	26.5	55.8	0.001311	0.199431
Day 1	$Slg^{Fe(II)-1stAN}$_D1_1stAN	23.9	22.3	n.d.	53.7	0.000959	0.141837
	$Slg^{Fe(II)-1stAN}$ _D1_AE	25.8	23.9	n.d.	50.3	0.004229	0.632625
	SlgFe(II)-1stAN _D1_2ndAN	24.6	24.3	n.d.	51.1	0.001615	0.228061
	$Slg^{Fe(II)-1stAN}$ _D1_ME	23.7	26.3	n.d.	50.0	0.001587	0.231449
Day 60	$Slg^{Fe(II)-1stAN}$ _D60_1stAN	14.0	52.5	n.d.	33.5	0.001139	0.178485
	$Slg^{Fe(II)-1stAN}$ _D60_AE	15.6	53.5	n.d.	30.9	0.00067	0.10915
	$Slg^{Fe(II)-1stAN}$ _D60_2ndAN	14.4	53.1	n.d.	32.5	0.000687	0.115002
	$Slg^{Fe(II)-1stAN}$ _D60_ME	14.9	52.9	n.d.	32.2	0.00083	0.137942
Day 110	$Slg^{Fe(II)-1stAN}$ _D110_1stAN	19.9	50.5	n.d.	29.6	0.000635	0.105201
	$Slg^{Fe(II)-1stAN}$ _D110_AE	20.2	51.7	n.d.	28.1	0.000638	0.106886
	$Slg^{Fe(II)-1stAN}$ _D110_2ndAN	20.8	50.8	n.d.	28.4	0.000713	0.107081
	$Slg^{Fe(II)-1stAN}$ _D110_ME	21.1	48.8	n.d.	30.1	0.000824	0.119101

[a] Statistical fit uncertainties generated from Athena for individual fractions were typically around 2-5%. "n.d.": not detected

Table 3. Mean percentages (± standard deviation) of Fe and P solid species present in sludge samples from different chambers of a well mixed pilot scale MBR at steady state.

	Fe-containing minerals present at steady state		
	Ferrihydrite	Fe-phosphate mineral	Lepidocrocite
Fe(II) dosing to membrane chamber	22.8 ± 3.1	43.4 ± 2.3	33.8 ± 1.9
Fe(II) dosing to 1st anoxic chamber	22.3 ± 2.2	38.2 ± 1.3	39.5 ± 2.0

	P-containing minerals present at steady state		
	P adsorbed	Fe-phosphate mineral	Phytic acid
Fe(II) dosing to membrane chamber	46.3 ± 0.6	27.1 ± 0.7	26.5 ± 0.8
Fe(II) dosing to 1st anoxic chamber	50.4 ± 1.2	20.5 ± 0.5	29.0 ± 1.0

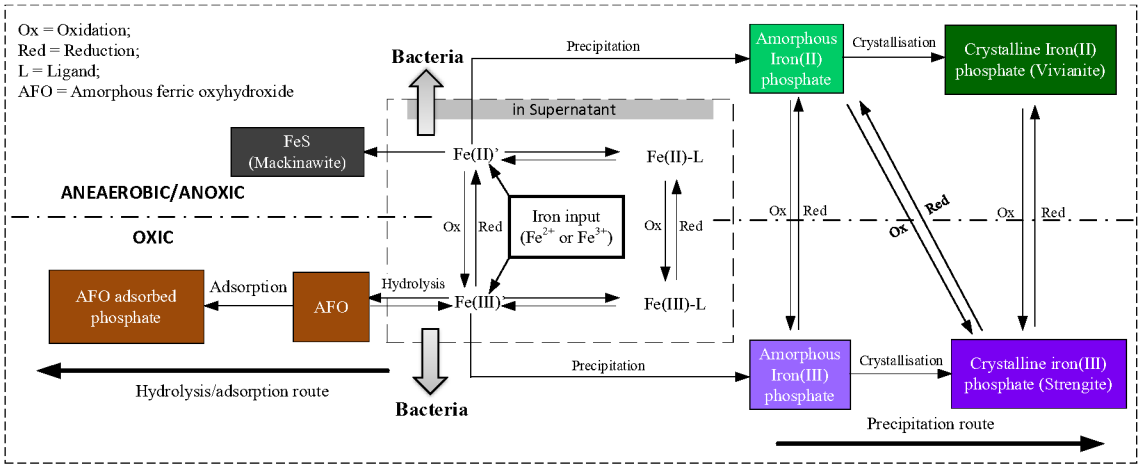

Figure 1. Schematic showing possible transformations in iron species following dosing of either ferrous (Fe^{2+}) or ferric (Fe^{3+}) salts to a membrane bioreactor. Solid forms of Fe are shown in colour. Adapted from Wang et al. 2014a.

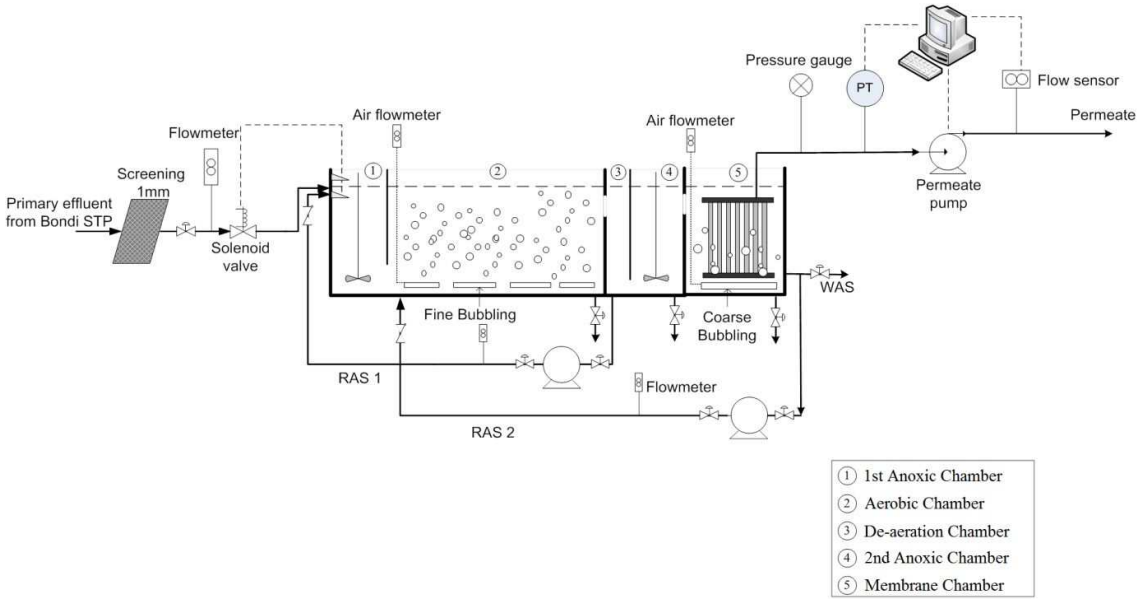

Figure 2. Schematic diagram of pilot scale MBR. Reproduced with permission from Wang et al. 2014b.

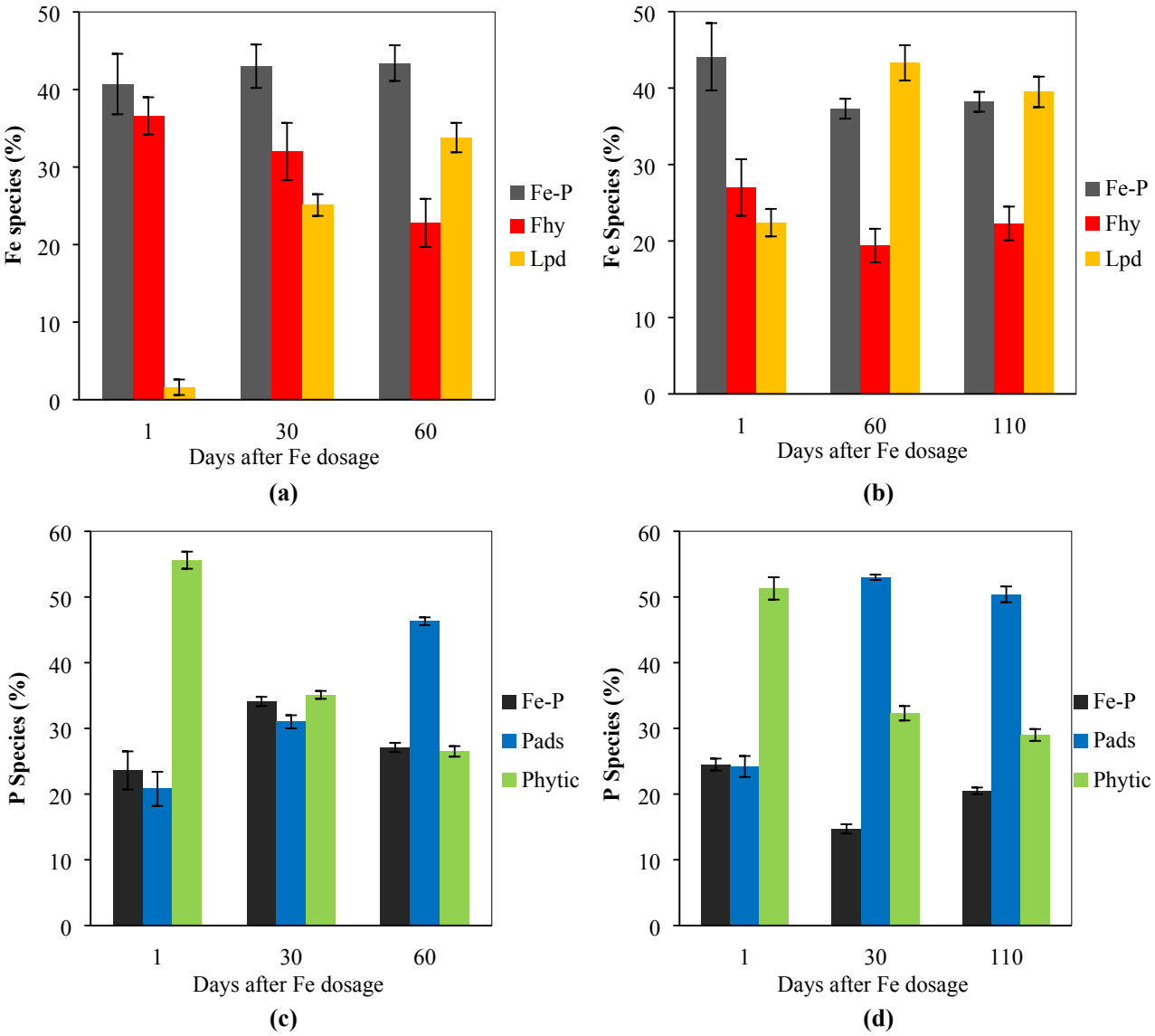

Figure 3. Evolution of fractions of Fe minerals and P species over time in pilot scale MBR; (a) Fe mineral distribution (%) with Fe dosed to Membrane Chamber; (b) Fe mineral distribution (%) with Fe dosed to 1st Anoxic Chamber; (c) P Species distribution (%) with Fe dosed to Membrane Chamber; (d) P Species distribution (%) with Fe dosed to 1st Anoxic Chamber. Fe-P: Fe(III)-Phosphate; Fhy: Ferrihydrite; Lpd: Lepidocrocite; Pads: P-adsorbed; Phytic: Phytic acid.

ToC Graphic

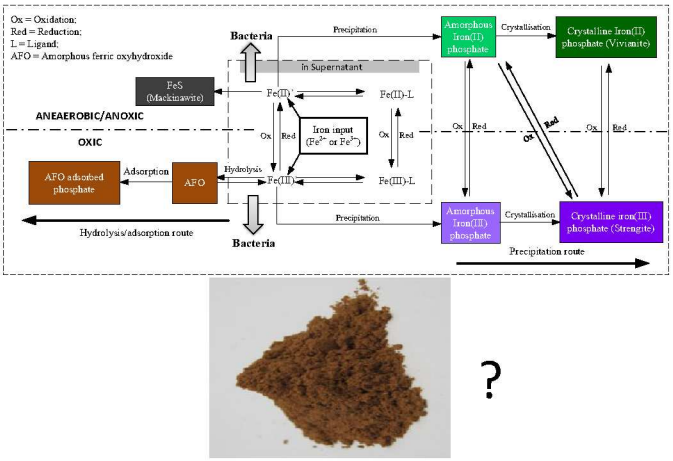
Ox = Oxidation;
Red = Reduction;
L = Ligand;
AFO = Amorphous ferric oxyhydroxide
Bacteria
Precipitation
Amorphous Iron(II) phosphate
Crystallisation
Crystalline Iron(II) phosphate (Vivianite)
In Supernatant
FeS (Mackinawite)
Fe(II)
Fe(II)-L
ANEAEROBIC/ANOXIC
OXIC
Ox
Red
Iron input (Fe^{2+} or Fe^{3+})
AFO adsorbed phosphate
Adsorption
AFO
Hydrolysis
Fe(III)
Fe(III)-L
Hydrolysis/adsorption route
Bacteria
Precipitation
Amorphous Iron(III) phosphate
Crystallisation
Crystalline iron(III) phosphate (Strengite)
Precipitation route

?